

Positron Emission Tomography for the Development and Characterization of Corneal Permanence of Ophthalmic Pharmaceutical Formulations

Anxo Fernández-Ferreiro,¹⁻⁴ Jesús Silva-Rodríguez,³ Francisco Javier Otero-Espinar,¹ Miguel González-Barcia,^{2,4} María Jesús Lamas,^{2,4} Alvaro Ruibal,^{3,5} Andrea Luaces-Rodríguez,¹ Alba Vieites-Prado,⁶ Tomas Sobrino,⁶ Michel Herranz,^{3,5} Lara García-Varela,³ José Blanco-Mendez,¹ María Gil-Martínez,⁷ María Pardo,⁸ Alexis Moscoso,³ Santiago Medín-Aguerre,⁹ Juan Pardo-Montero,^{3,10} and Pablo Aguiar^{3,5}

¹Pharmacy and Pharmaceutical Technology Department and Industrial Pharmacy Institute, Faculty of Pharmacy, University of Santiago de Compostela (USC), Campus Vida, Santiago de Compostela, Spain

²Pharmacy Department, Xerencia de Xestión Integrada de Santiago de Compostela (SERGAS), Travesía Choupana s/n Santiago de Compostela, Spain

³Molecular Imaging Group, Radiology Department, Universidade de Santiago de Compostela (USC) and Health Research Institute of Santiago de Compostela (IDIS), R/ San Francisco s/n, Santiago de Compostela, Spain

⁴Clinical Pharmacology Group, University Hospital, Santiago de Compostela (CHUS), Universidade de Santiago de Compostela, Health Research Institute of Santiago de Compostela (IDIS), Travesía da Choupana s/n Santiago de Compostela, Spain

⁵Nuclear Medicine Department and Molecular Imaging Group, University Hospital, Santiago de Compostela (CHUS), Universidade de Santiago de Compostela (USC), Health Research Institute of Santiago de Compostela (IDIS), Travesía da Choupana s/n Santiago de Compostela, Spain.

⁶Clinical Neurosciences Research Laboratory, University Hospital, Santiago de Compostela (CHUS), Universidade de Santiago de Compostela, Health Research Institute of Santiago de Compostela (IDIS), Travesía da Choupana s/n Santiago de Compostela, Spain

⁷Ophthalmology Department, Xerencia de Xestión Integrada de Santiago de Compostela (SERGAS), Travesía Choupana s/n Santiago de Compostela, Spain

⁸Obesidomic Group, Health Research Institute of Santiago de Compostela (IDIS), Travesía da Choupana s/n Santiago de Compostela, Spain

⁹Galician PET Radiopharmacy Unit, Galaria, University Hospital, Santiago de Compostela (CHUS), Travesía Choupana s/n Santiago de Compostela, Spain

¹⁰Medical Physics Department, University Hospital, Santiago de Compostela (CHUS), Travesía Choupana s/n Santiago de Compostela, Spain

Correspondence: Juan Pardo-Montero, Medical Physics Department, University Hospital, Santiago de Compostela (CHUS), Travesía Choupana s/n 15706 Santiago de Compostela, Spain; juan.pardo.montero@sergas.es.

Pablo Aguiar, Molecular Imaging Group, Radiology Department, Universidade de Santiago de Compostela (USC) and Health Research Institute of Santiago de Compostela (IDIS), R/ San Francisco s/n 15782, Santiago de Compostela, Spain; pablo.aguiar.fernandez@sergas.es.

AF-F and JS-R contributed equally to the work presented here and should therefore be regarded as equivalent authors.

Submitted: September 16, 2016

Accepted: November 29, 2016

Citation: Fernández-Ferreiro A, Silva-Rodríguez J, Otero-Espinar FJ, et al. Positron emission tomography for the development and characterization of corneal permanence of ophthalmic pharmaceutical formulations. *Invest Ophthalmol Vis Sci.* 2017;58:772-780. DOI:10.1167/iovs.16-20766

PURPOSE. This work is aimed at describing the utility of positron emission tomography/computed tomography (PET/CT) as a noninvasive tool for pharmacokinetic studies of biopermanence of topical ocular formulations.

METHODS. The corneal biopermanence of a topical ophthalmic formulation containing gellan gum and kappa carragenan (0.82% wt/vol) labeled with ¹⁸Fluorine (¹⁸F) radiotracers (¹⁸F-FDG and ¹⁸F-NaF) was evaluated by using a dedicated small-animal PET/CT, and compared with the biopermanence of an aqueous solution labeled with the same compounds. Regions of interest (ROIs) were manually drawn on the reconstructed PET images for quantifying the radioactivity concentration in the eye. The biopermanence of the formulations was determined by measuring the radioactivity concentration at different times after topical application. Additionally, cellular and ex vivo safety assays were performed to assess the safety of the performed procedures.

RESULTS. Differences were observed in the ocular pharmacokinetics of the two formulations. After 1.5 hours of contact, 90% of the hydrogel remained in the ocular surface, while only 69% of the control solution remained. Furthermore, it was observed that flickering had a very important role in the approach of the trial. The application of ¹⁸F-FDG in the eye was neither irritating nor cytotoxic for human corneal epithelial cells.

CONCLUSIONS. The use of small-animal PET and ¹⁸F radiotracers in ocular pharmacokinetics of ophthalmic formulations is feasible and could be a safe method for future ocular pharmacokinetic studies in humans.

Keywords: cell cytotoxicity, het cam, FDG, stimuli-responsive hydrogel, small-animal PET/CT



Interest in developing new drug delivery systems that increase ocular drug biopermanence has recently increased in ophthalmology research, mainly to overcome the high ocular clearance of conventional eye drops.¹ Increasing patients' adherence and establishing appropriate dosing schedules are key factors for improving treatment of many ophthalmic pathologies.²

Though the use of visible light to examine intraocular processes can be considered the oldest form of imaging in ophthalmology,³ the introduction of new imaging techniques has improved many aspects of both therapeutic/diagnostic ophthalmic procedures and the development of eye formulations and ophthalmic drugs. Nuclear magnetic resonance has been used for various purposes such as determining the pharmacokinetic profiles of drugs,⁴ studying corneal surface iontophoresis,⁵ or evaluating ocular surface biopermanence of ophthalmic hydrogels.⁶ Furthermore, other imaging techniques have been evaluated, such as gamma scintigraphy,^{7,8} real-time optical coherence tomography (OCT),⁹ and fluorophotometry.¹⁰

Positron emission tomography (PET) is a noninvasive imaging technique that visualizes the distribution of different radiotracers in the body, providing functional and molecular information on the tissues. The PET scanner detects pairs of gamma rays emitted from a molecule previously labeled with a radioactive isotope, usually ¹⁸Fluorine (¹⁸F). Afterward, three-dimensional images of the tracer concentration are obtained by reconstructing the acquired data.¹¹ Positron emission tomography is a relatively novel modality, mainly used for studying brain metabolism and cardiac function and for cancer detection.¹² However, PET is also emerging as a relevant modality for ophthalmology research, where it has been used in the diagnosis of primary ocular tumors and in neurophysiological studies.¹³⁻¹⁶

In this experimental study we present a novel methodology based on using PET for evaluating the biopermanence of ophthalmic drug delivery systems in the ocular surface. We used a small-animal PET/computed tomography (CT) scanner for studying the permanence of an ion-sensitive in situ hydrogel (smart hydrogel) composed of kappa carrageenan and gellan gum on the eye surface. Meanwhile, other parameters such as radiotracer delivery, corneal permeation, security, and irritating cytotoxic radiotracers were also studied.

MATERIALS AND METHODS

In Vitro and Ex Vivo Assays

Ion-Sensitive Hydrogel With Radiotracers. An ion-sensitive hydrogel based on gellan gum and kappa-carrageenan was prepared with an overall total polymer concentration of 0.82% (wt/vol), consisting of 80% gellan gum and 20% kappa-carrageenan. Deacylated gellan gum (GG) (Kelcogel CG-LA) and kappa-carrageenan (CK) (GENUGEL carrageenan GC-130) were a generous gift of CP Kelco (Levallois-Perret, France). The hydrogel preparation method and their properties were described in our previous work.⁶ Two radiotracers were incorporated into the hydrogel: ¹⁸F-sodium fluoride (¹⁸F-NaF) and ¹⁸F-fluorodeoxyglucose (¹⁸F-FDG). One hundred microliters of each radiotracer was incorporated in 1 mL each hydrogel until homogenization. To test the uniformity of the radiotracer in the labeled hydrogel, 10 samples of 10 μ L hydrogel were randomly taken from each formulation and measured using a high-precision dose calibrator (Atomlab 500; Biodex Medical Systems, Inc., New York, NY, USA).

In order to characterize the labeling stability of the hydrogel with the radiotracer, the loss of radiotracer from hydrogels in

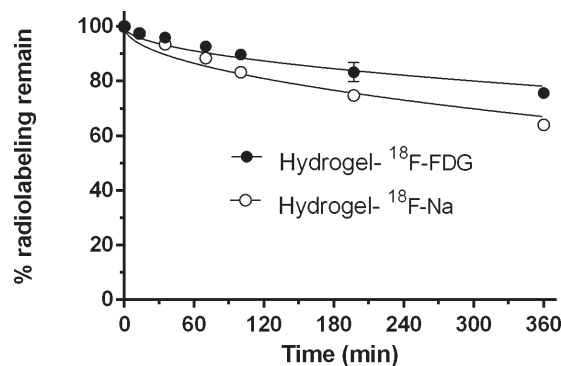


FIGURE 1. Elimination of ¹⁸F-FDG and ¹⁸F-Na from the hydrogel versus time.

the presence of simulated eye tears (SLF) was estimated by using Franz diffusion cells with GVS (Barcelona, Spain) 0.20- μ m cellulose acetate membranes (membrane surface area of 0.785 cm²). The donor compartment is SLF (375 μ L) and 1 mL hydrogel. Sink conditions were obtained in the receptor compartment with SLF, with a volume of the receptor fluid of 6 mL. During the experiment, the receptor compartment was continuously homogenized using an incubating orbital shaker (VWR International Eurolab S.L., Barcelona, Spain) at 200 rpm and 33°C. Serial sampling was performed after 10, 20, 30, 60, 90, 120, and 300 minutes. Each experiment was repeated three times. Simulated eye tears were prepared as previously detailed by Ceulemans and Ludwig.¹⁷ The following equation, derived from Fick's second law, was employed to estimate the radiotracer's diffusivity in the hydrogel (D):

$$\frac{Q_t}{Q_\infty} = 4 \cdot \sqrt{\left(\frac{D \cdot t}{\pi \cdot b^2}\right)}$$

where Q_t represents the quantity of radiolabel diffused at time t , Q_∞ the total quantity of radiolabel diffused at the end of the experiment, and b the thickness of the layer of hydrogel. D values were obtained through a nonlinear fit using GraphPad Prism 6.0 software (2014; GraphPad Software, Inc., San Diego, CA, USA).

Radiotracer "Ex Vivo" Corneal Permeability. In order to ensure that the radiotracers did not cross the cornea, permeation studies were conducted. Rat eyes were obtained during the first hour after the animal's death and transported following the Bovine Corneal Opacity and Permeability (BCOP) test protocol.¹⁸ Once received, the corneas were isolated with 2 to 3 mm of surrounding sclera, washed with an isotonic saline solution, and mounted on Franz diffusion cells. The receptor chamber was filled (6 mL) with SLF. The cornea was placed on the receptor chamber, and finally the donor chamber was fixed and filled with SLF (area available for permeation: 0.049 cm²). During the experiment, the receptor compartment was continuously homogenized using the VWR incubating orbital shaker at 200 rpm and 33°C. Serial sampling was performed after 10, 20, 30, 60, 90, 120, and 300 minutes. Each experiment was repeated three times.

Cell Cytotoxicity Assay. The influence of the radioactivity on the cell viability of ATCC (Manassas, Virginia) normal human primary corneal epithelial cells (HCE) was studied by using the xCELLigence Real-Time Cell Analyzer System (RTCA) (ACEA Biosciences, San Diego, CA, USA) for real-time monitoring. Cell index (CI)¹⁹ was used to represent the number of cells based on the measured electric impedance. Three thousand cells per well (16-well E-plates) were incubated for 24 hours. Subsequently, the original culture

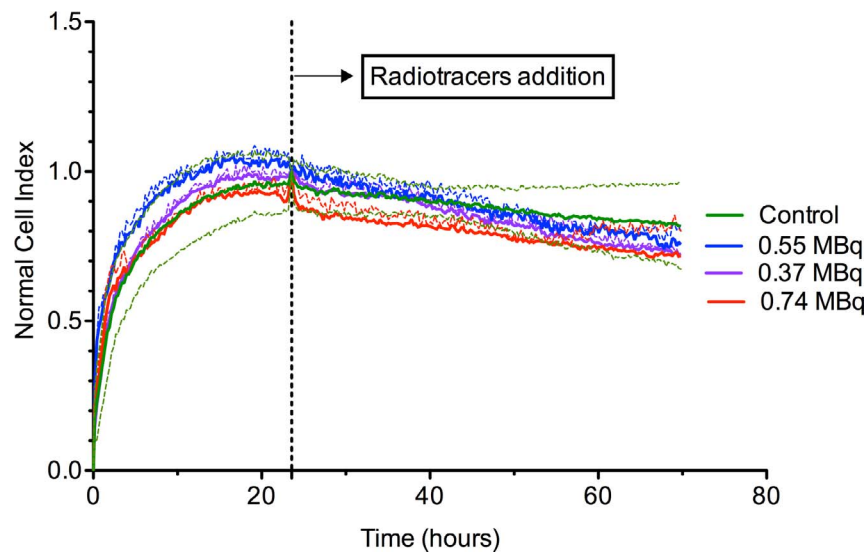


FIGURE 2. Kinetics of growth of HCE in contact with different radioactivities of ¹⁸F-FDG using RTCA. Mean (—) and standard deviation (⋯); n = 4.

medium was aspirated and different ¹⁸F-FDG radioactivities (0.37, 0.55, and 0.74 MBq) were added to different wells. The results were represented as dose-response curves versus time, and normalized CI (NCD) was calculated.²⁰

Ocular Irritation Assay. Hen's egg test chorion allantoic membrane (HET-CAM)²¹ was used to study the acute ocular irritability using the methodology described in our previous work.²² A volume of 0.3 mL pure ¹⁸F-FDG and ¹⁸F-FDG-hydrogel dispersion was tested and compared with positive control (NaOH 0.1 N). Three eggs were used for each compound. Blood vessels were observed for 300 seconds with a stereomicroscope (Olympus Iberia, Barcelona, Spain), looking for episodes of bleeding, coagulation, and partial lysis. The irritation index (IS) was determined as described in Protocol INVITTOX 96.²³ To quantify the extent of the damage of the chorion allantoic membrane caused by treatments, a modification of the method described by McKenzie et al.²⁴ was also used. Photographs of the egg membrane were taken at different times of treatment using the Olympus SZ-60 stereomicroscope and SC100 camera. Photographs were taken using an aperture of f1, a shutter speed of 1/3 second, and a size of 3840 × 2748 pixels. The images were converted to 16-bit grayscale and finally analyzed using ImageJ software (<http://imagej.nih.gov/ij/>; provided in the public domain by the National Institutes of Health, Bethesda, MD, USA). To analyze the image the menu option "square" was used, selecting the entire image, and the average gray pixel value profile was plotted by selecting ALT K.

In Vivo Evaluation of Biopermanence Time of Hydrogel in the Ocular Surface

Animals. This study was carried out on male Sprague-Dawley rats with an average weight of 300 g supplied by the animal facility at the University of Santiago Compostela. During the experiment, the animals were kept in individual cages with free access to food and water in a room under controlled temperature (22 ± 1°C) and humidity (60 ± 5%) conditions and with day/night cycles regulated by artificial light (12/12 hours). The animals were treated according to the ARVO Statement for the Use of Animals in Ophthalmic and Vision Research and the Guide for the Care and Use of Laboratory Animals.^{25,26} Experiments were approved by the Galician Network Committee for Ethics Research following the Spanish

and European Union (EU) rules (86/609/CEE, 2003/65/CE, 2010/63/EU, RD 1201/2005 and RD53/2013).

PET Experimental Procedure. Positron emission tomography imaging and CT images were acquired using the Albira PET/CT Preclinical Imaging System (Bruker Biospin, Woodbridge, CT, USA). The PET subsystem comprises three rings of eight compact modules based on monolithic crystals coupled to multianode photomultiplier tubes (MAPMTs), forming an octagon with an axial field of view (FOV) of 40 mm per ring and a transaxial FOV of 80 mm in diameter, while the computed tomography (CT) system comprises a commercially available microfocus x-ray tube and a CsI scintillator two-dimensional pixelated flat-panel x-ray detector.

Before PET experiments, the animals were placed in a gas chamber containing 2% isoflurane in oxygen. When unconscious, the animals were taken from the chamber and kept under anesthesia, administered via a mask, during the experiment (1.5% isoflurane in oxygen). Anesthetized animals were positioned in the PET bed, and 7.5 μL radiotracer solution or 7.5 μL hydrogel-radiotracer was instilled into the conjunctival sac eye using a pipette. The administered radioactivity was 0.37 ± 0.08 MBq. After the instillation, dynamic PET images were obtained, resulting in 15-minute frames during 1.5 hours. Three different conditions were tested: (1) image acquisition starting immediately after instillation while the animal was asleep; (2) image acquisition starting 1.5 hours after instillation, with the animal kept awake in its cage during the waiting time; and (3) image acquisition starting 3 hours after instillation, again with the animal awake during that period. After instillation, the eyelids were gently moved for distribution of the radiolabeled formulation.

In order to evaluate the flickering effect, additional studies were performed with awakened animals, acquiring single frames of 5 minutes every 45 minutes (animals were anesthetized only during the PET acquisition). Four animals (eight eyes) were tested for each condition.

TABLE. Fitting Parameters of the Experimental Data to a Diffusion Kinetics Model

Radiotracer	D, cm ² ·min ⁻¹	R ²
¹⁸ F-Na	5.3·10 ⁻² ± 0.12·10 ⁻²	0.895–0.950
¹⁸ F-FDG	2.3·10 ⁻² ± 0.46·10 ⁻²	0.974–0.932

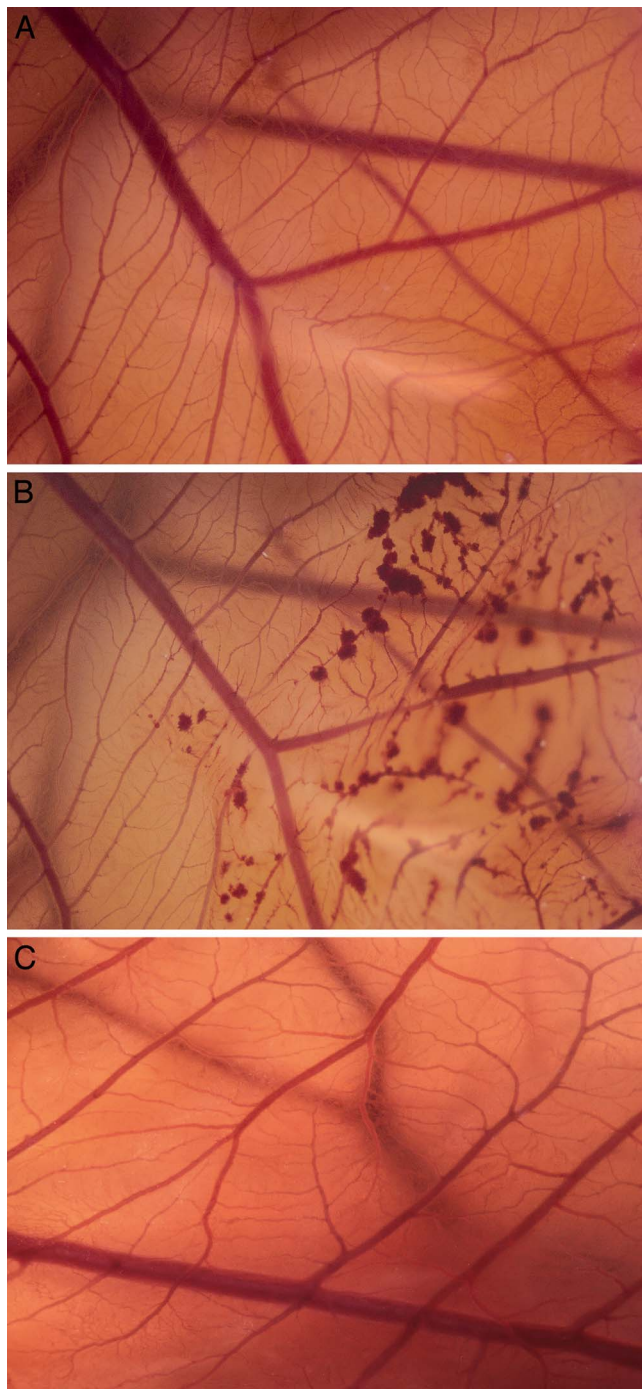


FIGURE 3. HET-CAM assay after 5 minutes of contact with (A) ^{18}F -FDG (B) positive control (NaOH 0.1 N), and (C) ^{18}F -FDG-hydrogel dispersion.

PET Data Analysis. Scatter and random coincidences were corrected by using the protocols implemented in the scanner. Attenuation correction was not performed. Images were reconstructed by using the maximum likelihood expectation maximization (MLEM) algorithm. Twelve iterations were performed with a reconstructed image pixel size of $0.4 \times 0.4 \times 0.4 \text{ mm}^3$. After reconstruction, quantitative measurements were obtained using the MRICro software package (University of South Carolina, Columbia, SC, USA). Different regions of interest (ROIs) were manually drawn containing the signal on each eye. The ROIs were replicated on the different frames

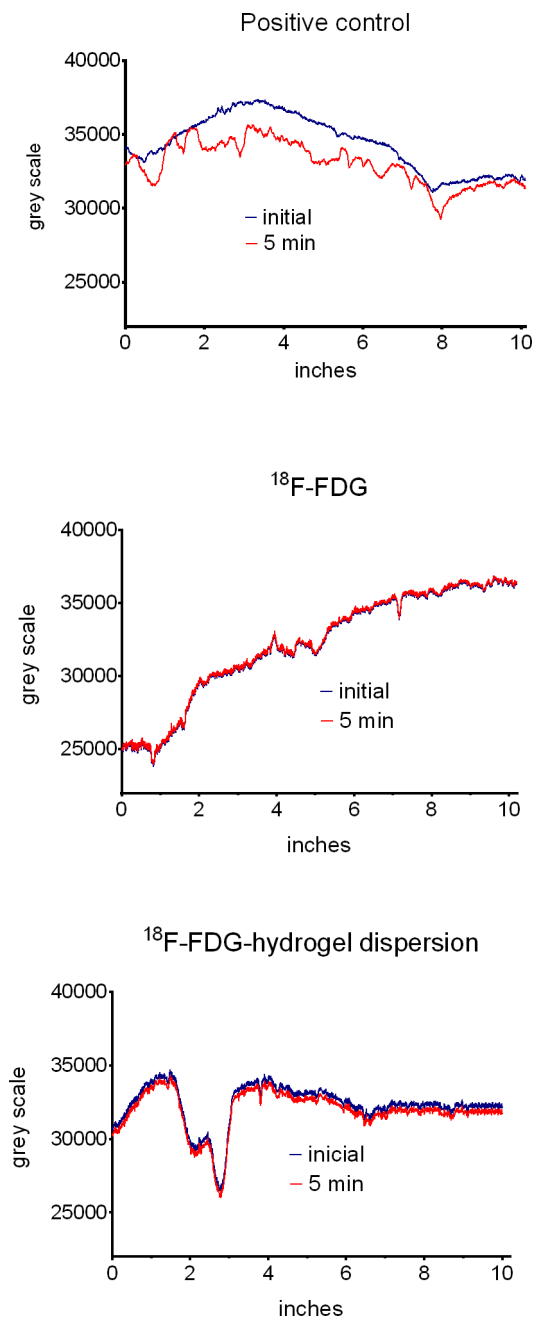


FIGURE 4. Plot of the pixel gray value of HET-CAM images over distance for each of the test solutions.

over time, and the results were corrected for radioactive decay. Afterward, graphical representations of radioactivity versus time were obtained.

RESULTS

Radiotracer in Hydrogel

The uniformity study showed a largely homogeneous distribution of the radiotracers in the hydrogel (average $1.20 \mu\text{Ci}/\mu\text{L}$; $\text{SD} = 0.017$; coefficient of variation [CV] 1.45).

The hydrogel tested in this work underwent rapid gelation upon contact with simulated tear fluid, and this gelation allowed the retention of the radiotracers in it for long periods

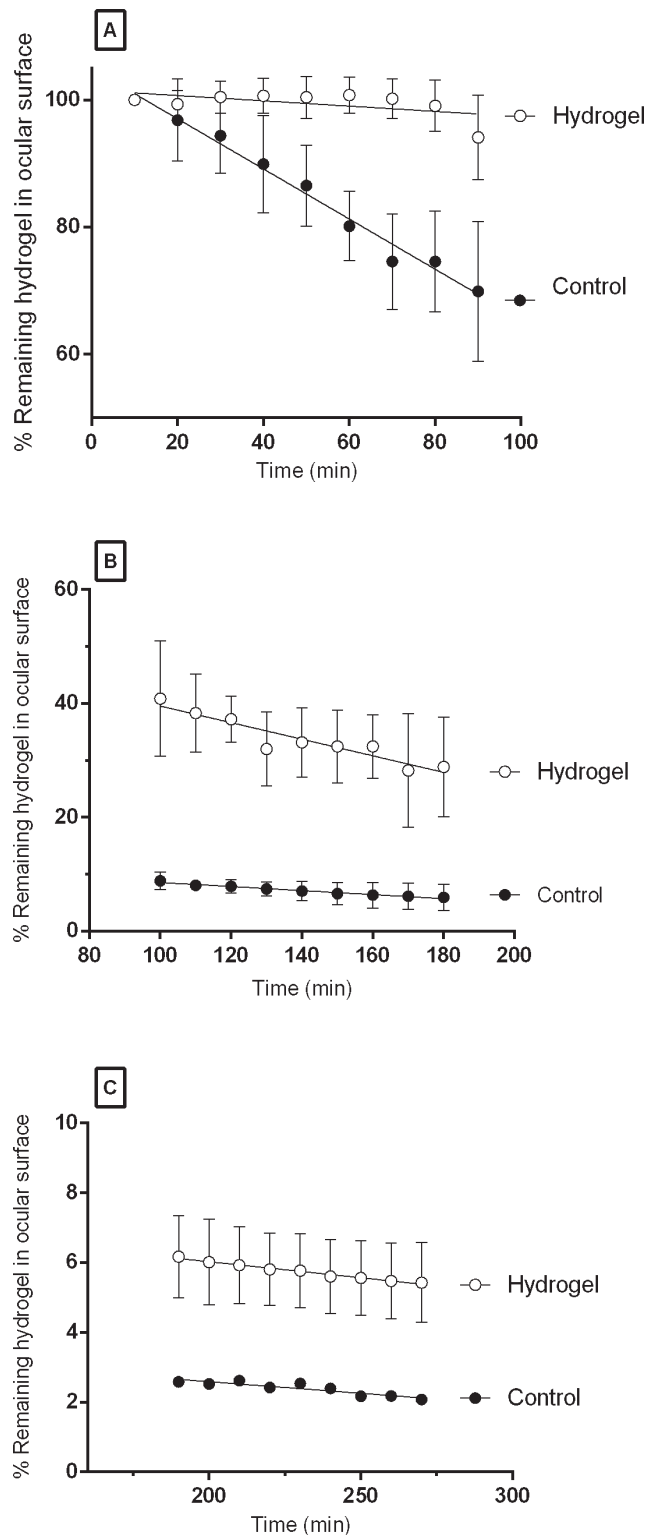


FIGURE 5. Dynamic study with anesthetized animals. Kinetic profile of hydrogel (blank circles) and control solution (solid circles) in three different conditions. (A) During 1.5 hours post instillation, (B) at 1.5 hours post instillation, and (C) 3 hours post instillation.

of time. Figure 1 shows the loss of radiotracers versus time from the ion-sensitive hydrogels containing the ^{18}F and ^{18}F -FDG. The Table shows the results of the fit of the experimental data to the Higuchi kinetics model.²⁷ The good fits obtained

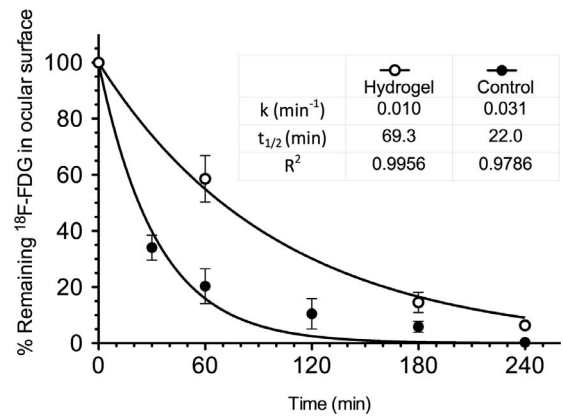


FIGURE 6. Dynamic study with awake animals. Kinetic profile of hydrogel (blank circles) and control solution (solid circles).

suggest that loss of the radiotracer is caused by diffusion across the hydrogel network.

The hydrogel contained 76% of the ^{18}F -FDG 360 minutes post preparation, while the presence of ^{18}F -NaF after the same time was just 65%. Two-way analysis of variance indicated that significant differences existed ($\alpha < 0.01$, Sidak multiple comparison test) between the two compounds from 60 minutes onward. Based on these results, we decided to use ^{18}F -FDG for the biopermanence assays. On the other hand, no diffusion of the radiotracers through the cornea was found in our cornea permeability studies. This is an essential result as it guarantees that the radioactivity values measured in the biopermanence assays are indeed in the hydrogel and not accumulated beyond the cornea.

Ocular Safety Studies

Normalized cell index values obtained from the real-time monitoring are shown in Figure 2. It can be seen that treated and untreated HCE show similar growth kinetics, indicating that the tested radioactivity levels are not cytotoxic and allow normal growth of corneal epithelial cells. On the other hand, Figures 3 and 4 show that the use of radiotracer is not irritating. The value of the IS index of zero for both radiotracers, as well as the distribution of gray pixel levels in the HET-CAM images before and after treatments, indicates that no alterations were produced in the membrane. The presence of a severe hemorrhage produces dark areas in the HET-CAM images, which leads to a significant decrease in the gray scale values, as can be seen for the positive control in Figure 4A. This is an important factor since the administration of an irritating compound can alter flickering, thus compromising the biopermanence results.

Biopermanence Time of Hydrogel in the Ocular Surface

The biopermanence of the hydrogel labeled with ^{18}F -FDG was evaluated by using small-animal PET imaging in rats and compared to a saline solution containing ^{18}F -FDG as control formulation. For both formulations, a strong signal at early times after instillation was observed. Figure 5A shows the disappearance of the formulations in anesthetized animals (no blinking). It can be seen that after 1.5 hours of contact, 90% of the hydrogel remained in the ocular surface, while only 69% of the control solution remained. The flickering effect can be clearly seen in Figure 5B, with just 40% of the hydrogel still on the eye surface at 1.5 hours after instillation in animals that

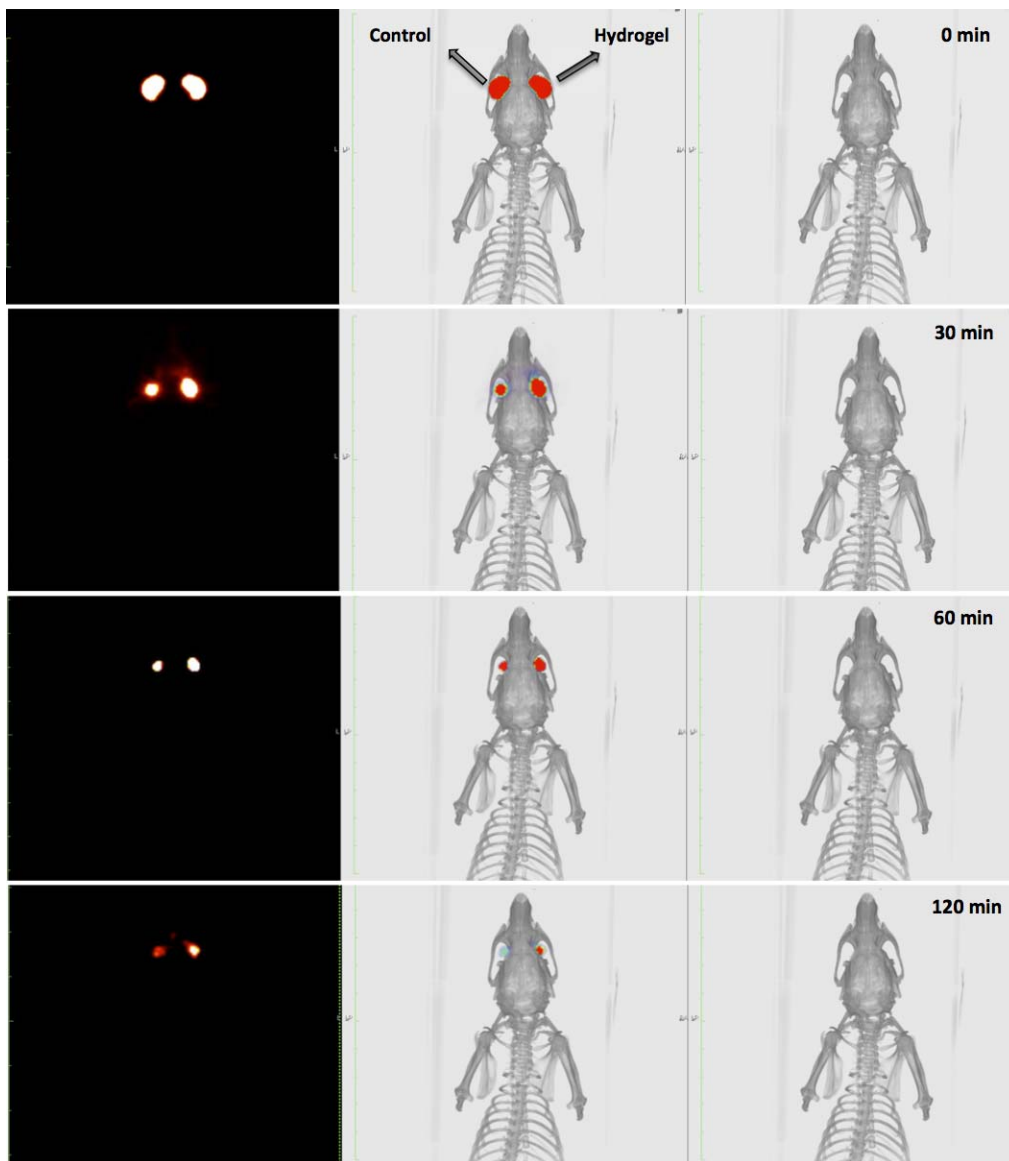


FIGURE 7. PET (left), CT (right), and PET/CT fused image (center). The difference between the signal in the eye with hydrogel and the control eye can be observed over time (0-120 minutes).

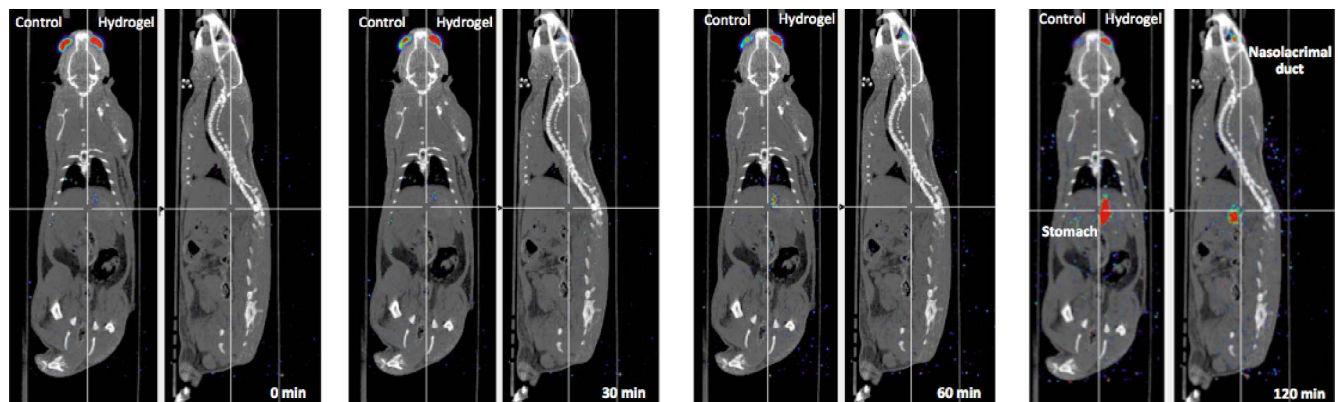


FIGURE 8. Fused whole-body PET/CT images (coronal and sagittal views) over time (0-120 minutes). It can be observed that the signal decreases in the eyes while increasing at systemic level (stomach).

were awake during that period (versus 90% in the absence of blinking from Fig. 5A). A similar situation was seen with the control solution, with only 10% of the saline remaining on the eye after 1.5 hours (versus 70% in the absence of blinking). It seems that the flickering effect on the biopermanence time for control was greater than for the hydrogel solutions. Under the same conditions but using longer contact times (3 hours), 6% of the hydrogel remained, while the presence of the control solution was practically nonexistent, as shown in Figure 5C. The experiments with anesthetized animals, with no blinking, showed that the biopermanence linearly decreased with time. However, when the animal was kept awake after the instillation until acquisition, the linear relationship no longer held. In this scenario, which more accurately resembles a clinical situation, the biopermanence on the eye surface follows an exponential dependence on time, as seen in Figure 6. We obtained average lifetimes of 69.3 minutes in the case of the hydrogel and 22 minutes for the control solution.

The latter results are clearly illustrated in other images. Figure 7 shows that the signal decreases over time in the eyes, mainly in the control eye. In addition, Figure 8 shows that such signal decrease is associated with a signal increase at the systemic level.

DISCUSSION

The development of new ophthalmic topical vehicles to increase the permanence of drugs on the ocular surface is essential to improve adherence and therapeutic efficacy of ocular drugs.²⁸ Regarding this, new noninvasive and safe methodologies are required to provide accurate information on the residence time of a formulation on the ocular surface, which is a key factor for establishing optimal dosage regimens.²⁹

To date, several methodologies have been proposed to carry out biopermanence study of ophthalmic formulations. First, a novel methodology was proposed by our group based on magnetic resonance imaging (MRI) technology.⁶ In such a study, only qualitative measures are made regarding the biopermanence of ion-sensitive hydrogels, without providing pharmacokinetic profiles. It has to be mentioned that, despite the high availability of MRI scanners in hospitals, the use of this technology to perform high-resolution studies in rat eyes requires the development of specific antennas and dedicated software for data analysis.^{4,30}

On the other hand, methodologies based on fluorescent markers have shown that ophthalmic formulations containing hyaluronic acid and chitosan increase ocular biopermanence over control markers.^{10,31} Furthermore, increased residence times have also been observed in other ion-sensitive hydrogels using microcapillary and scintigraphy studies.^{32,33}

In this work, we propose an alternative novel methodology based on PET technology, and the use of low half-life radiotracers is described. However, direct comparison between our results and those obtained from the previously proposed methodologies is complicated, due to the different composition and concentration of the polymers that form hydrogels, the different methodologies used in each study, and the different species employed.^{34,35} In any case, it must be mentioned that PET has greater sensitivity and provides three-dimensional images that can improve the interpretation of images with respect to previous methodologies, more importantly when considering fusion with CT images,³⁶ as proposed in our work. Furthermore, due to the greater sensitivity in PET technology, it should be noted that the radioactivity levels used in our biopermanence studies are much smaller than those

used in other pharmacokinetic studies, which use radioisotopes with long half-life, such as ¹²⁴I (10 MBq, half-life = 4.17 days)³⁷ (Dangl D, et al. *IOVS* 2009;50:ARVO E-Abstract 3689) or ^{99m}Tc (1 MBq, half-life = 6 hours).³⁸ However, clinical implementation of a biopermanence assay based on our methodology would require a careful assessment of radiation protection issues in the patient. The radiation dose deposited in the stomach or other systemic organs is negligible when considering the activities used in our work. We would like to point out that standard PET studies use an activity of 555 MBq, over one hundred times larger than those employed in our work. This supports the contention that the systemic dose in our study is clearly negligible. Instead, the eye lens might be the most limiting structure, as it is very radiation sensitive. There is evidence of radiation doses of approximately 2 Gy leading to the development of cataracts,³⁹ and there is a strong limit on the dose to the eye lens for both exposed staff and the general public. As a preliminary result, a calculation of the dose delivered to the eye lens in a clinical study using the same radioactivity levels employed in our preclinical study provided values of radiation doses in the range of 10 to 20 mGy, which seem to be significantly below the dose limits. Furthermore, we found that the radioactivity levels of ¹⁸F-FDG used do not affect the viability of human epithelial cells and do not cause eye irritation. Also it should be noted that no diffusion of ¹⁸F-FDG through the cornea was found in our work. The latter result is also essential to ensure accurate determination of the biopermanence of the hydrogel in the eye, since if such diffusion happened, the observed signal would partially be due to radioactivity trapped beyond the cornea.^{40,41}

Finally, we recommend the use of dynamic protocols considering awake animals as long as possible, thus ensuring greater flicker and therefore a more realistic situation in humans. It must be mentioned that although human subjects exhibited a higher average blink rate than rats, the temporal pattern of spontaneous blinking was qualitatively similar for both species.⁴²

We can conclude that the proposed methodology seems feasible for conducting preclinical comparative studies on corneal permanence of different formulations of hydrogels. In contrast, its use in clinical trials to establish dosages will require extensive studies to ensure that the radiotracers are not trapped beyond the human cornea.

Acknowledgments

Supported by Instituto de Salud Carlos III (Rio Hortega Research Grant CM15/00188 [AF-F]) and Miguel Servet Research Grant CP12/03162 (JP-M), Ramón y Cajal (RYC-2015-17430 fellowship [PA]); Fundación Mutua Madrileña and Fundación Española Farmacia Hospitalaria (AISEFH); Xunta de Galicia (Department of Education, GRC2014/027) and the European Union program FEDER. TS (CP12/03121) is recipient of a research contract from Miguel Servet Program of Instituto de Salud Carlos III. The funders had no role in the design, data collection and analysis, decision to publish, or preparation of the manuscript.

Disclosure: **A. Fernández-Ferreiro**, None; **J. Silva-Rodríguez**, None; **F.J. Otero-Espinar**, None; **M. González-Barcia**, None; **M.J. Lamas**, None; **A. Ruibal**, None; **A. Luaces-Rodríguez**, None; **A. Vieites-Prado**, None; **T. Sobrino**, None; **M. Herranz**, None; **L. García-Varela**, None; **J. Blanco-Mendez**, None; **M. Gil-Martínez**, None; **M. Pardo**, None; **A. Moscoso**, None; **S. Medfín-Aguerre**, None; **J. Pardo-Montero**, None; **P. Aguiar**, None

References

- Almeida H, Amaral MH, Lobão P, Lobo JMS. In situ gelling systems: a strategy to improve the bioavailability of ophthalmic

- mic pharmaceutical formulations. *Drug Discov Today*. 2014; 19:400–412.
2. Patel A, Cholkar K, Agrahari V, Mitra AK. Ocular drug delivery systems: an overview. *World J Pharmacol*. 2013;2:47–64.
 3. Eter N. Molecular imaging of the eye. *Br J Ophthalmol*. 2010; 94:1420–1426.
 4. Li SK, Lizak MJ, Jeong E-K. MRI in ocular drug delivery. *NMR Biomed*. 2008;21:941–956.
 5. Li SK, Jeong E-K, Hastings MS. Magnetic resonance imaging study of current and ion delivery into the eye during transscleral and transcorneal iontophoresis. *Invest Ophthalmol Vis Sci*. 2004;45:1224–1231.
 6. Fernández-Ferreiro A, González Barcia M, Gil-Martínez M, et al. In vitro and in vivo ocular safety and eye surface permanence determination by direct and Magnetic Resonance Imaging of ion-sensitive hydrogels based on gellan gum and kappa-carrageenan. *Eur J Pharm Biopharm*. 2015;94:342–351.
 7. Felt O, Furrer P, Mayer JM, Plazonnet B, Buri P, Gurny R. Topical use of chitosan in ophthalmology: tolerance assessment and evaluation of precorneal retention. *Int J Pharm*. 1999;180:185–193.
 8. Gupta H, Aqil M, Khar RK, et al. Development and characterization of 99mTc-timolol maleate for evaluating efficacy of on situ ocular drug delivery system. *AAPS PharmSciTech*. 2009;10:540–546.
 9. Wang J, Aquavella J, Palakuru J, Chung S. Repeated measurements of dynamic tear distribution on the ocular surface after instillation of artificial tears. *Invest Ophthalmol Vis Sci*. 2006;47:3325–3329.
 10. Mochizuki H, Yamada M, Hatou S, Tsubota K. Turnover rate of tear-film lipid layer determined by fluorophotometry. *Br J Ophthalmol*. 2009;93:1535–1538.
 11. Lameka K, Farwell MD, Ichise M. Positron emission tomography. *Handb Clin Neurol*. 2016;135:209–227.
 12. Bengel FM, Higuchi T, Javadi MS, Lautamäki R. Cardiac positron emission tomography. *J Am Coll Cardiol*. 2009;54: 1–15.
 13. Sek K, Wilson D, Paton K, Benard F. The role of 18F-FDG PET/CT in assessment of uveal melanoma and likelihood of primary tumour visualisation based on AJCC tumour size. *J Nucl Med*. 2016;57(suppl 2):409.
 14. García-Rojas L, Adame-Ocampo G, Alexánder E, Tovilla-Canales JL. 18-Fluorodeoxyglucose uptake by positron emission tomography in extraocular muscles of patients with and without Graves' ophthalmology. *J Ophthalmol*. 2013;2013: 529187.
 15. Christoforidis JB, Carlton MM, Knopp MV, Hinkle GH. PET/CT imaging of I-124-radiolabeled bevacizumab and ranibizumab after intravitreal injection in a rabbit model. *Invest Ophthalmol Vis Sci*. 2011;52:5899–5903.
 16. Wang W-F, Ishiwata K, Kiyosawa M, et al. Investigation of the use of positron emission tomography for neuroreceptor imaging in rabbit eyes. *Ophthalmic Res*. 2004;36:255–263.
 17. Ceulemans J, Ludwig A. Optimisation of carbomer viscous eye drops: an in vitro experimental design approach using rheological techniques. *Eur J Pharm Biopharm*. 2002;54: 41–50.
 18. OECD. Test No. 437: Bovine Corneal Opacity and Permeability Test Method for Identifying Ocular Corrosives and Severe Irritants. Paris: Organisation for Economic Co-operation and Development; 2009. Available at: <http://www.oecd-ilibrary.org/content/book/9789264076303-en>. Accessed January 28, 2014.
 19. Xing JZ, Zhu L, Gabos S, Xie L. Microelectronic cell sensor assay for detection of cytotoxicity and prediction of acute toxicity. *Toxicol In Vitro*. 2006;20:995–1004.
 20. Atienza JM, Zhu J, Wang X, Xu X, Abassi Y. Dynamic monitoring of cell adhesion and spreading on microelectronic sensor arrays. *J Biomol Screen*. 2005;10:795–805.
 21. Fernández-Ferreiro A, González Barcia M, Gil Martínez M, Blanco Mendez J, Lamas Díaz MJ, Otero Espinar FJ. Analysis of ocular toxicity of fluconazole and voriconazole eyedrops using HET-CAM [in Spanish]. *Farm Hosp*. 2014;38:300–304.
 22. Fernández-Ferreiro A, Fernández Bargiela N, Varela MS, et al. Cyclodextrin-polysaccharide-based, in situ-gelled system for ocular antifungal delivery. *Beilstein J Org Chem*. 2014;10: 2903–2911.
 23. Hen's Egg Test on the Chorioallantoic Membrane (HET-CAM) INVITTOX n° 96. Available at: <http://www.vitrotox.com/uploadfile/UploadFile/2008121382926916.pdf>. Accessed January 27, 2014.
 24. McKenzie B, Kay G, Matthews KH, Knott RM, Cairns D. The hen's egg chorioallantoic membrane (HET-CAM) test to predict the ophthalmic irritation potential of a cysteamine-containing gel: quantification using Photoshop® and ImageJ. *Int J Pharm*. 2015;490:1–8.
 25. The Association for Research in Vision and Ophthalmology. Statement for the Use of Animals in Ophthalmic and Visual Research. Available at: http://www.arvo.org/About_ARVO/Policies/Statement_for_the_Use_of_Animals_in_Ophthalmic_and_Visual_Research/. Accessed December 10, 2016.
 26. National Research Council (US) Committee for the Update of the Guide for the Care and Use of Laboratory Animals. *Guide for the Care and Use of Laboratory Animals*. 8th ed. Washington, DC: National Academies Press; 2011.
 27. Siepmann J, Peppas NA. Higuchi equation: derivation, applications, use and misuse. *Int J Pharm*. 2011;418:6–12.
 28. Thompson AC, Thompson MO, Young DL, et al. Barriers to follow-up and strategies to improve adherence to appointments for care of chronic eye diseases. *Invest Ophthalmol Vis Sci*. 2015;56:4324–4331.
 29. Gomes CM, Abrunhosa AJ, Ramos P, Pauwels EKJ. Molecular imaging with SPECT as a tool for drug development. *Adv Drug Deliv Rev*. 2011;63:547–554.
 30. Alikacem N, Yoshizawa T, Nelson KD, Wilson CA. Quantitative MR imaging study of intravitreal sustained release of VEGF in rabbits. *Invest Ophthalmol Vis Sci*. 2000;41:1561–1569.
 31. Meadows DL, Paugh JR, Joshi A, Mordaunt J. A novel method to evaluate residence time in humans using a nonpenetrating fluorescent tracer. *Invest Ophthalmol Vis Sci*. 2002;43:1032–1039.
 32. Liu Y, Liu J, Zhang X, Zhang R, Huang Y, Wu C. In situ gelling gelrite/alginate formulations as vehicles for ophthalmic drug delivery. *AAPS PharmSciTech*. 2010;11:610–620.
 33. Greaves JL, Wilson CG, Rozier A, Grove J, Plazonnet B. Scintigraphic assessment of an ophthalmic gelling vehicle in man and rabbit. *Curr Eye Res*. 1990;9:415–420.
 34. Kashikar VS, Gonjari ID. In situ gelling systems of ofloxacin: comparative performance of in vivo precorneal drainage and pharmacokinetic study. *Asian J Pharm*. 2013;7:15–20.
 35. Rupenthal ID, Green CR, Alany RG. Comparison of ion-activated in situ gelling systems for ocular drug delivery. Part 2: Precorneal retention and in vivo pharmacodynamic study. *Int J Pharm*. 2011;411:78–85.
 36. Rahmim A, Zaidi H. PET versus SPECT: strengths, limitations and challenges. *Nucl Med Commun*. 2008;29:193–207.
 37. Kuntner C, Wanek T, Hoffer M, et al. Radiosynthesis and assessment of ocular pharmacokinetics of 124I-labeled chitosan in rabbits using small-animal PET. *Mol Imaging Biol*. 2011;13:222–226.
 38. Snibson GR, Greaves JL, Soper NDW, Prydal JI, Wilson CG, Bron AJ. Precorneal residence times of sodium hyaluronate

- solutions studied by quantitative gamma scintigraphy. *Eye*. 1990;4:594-602.
39. Ainsbury EA, Bouffler SD, Dörr W, et al. Radiation cataractogenesis: a review of recent studies. *Radiat Res*. 2009;172:1-9.
 40. Novack GD, Moyer ED. How much nonclinical safety data are required for a clinical study in ophthalmology? *J Ocul Pharmacol Ther*. 2016;32:5-10.
 41. Ng S-F, Rouse JJ, Sanderson FD, Meidan V, Eccleston GM. Validation of a static Franz diffusion cell system for in vitro permeation studies. *AAPS PharmSciTech*. 2010;11:1432-1441.
 42. Kaminer J, Powers AS, Horn KG, Hui C, Evinger C. Characterizing the spontaneous blink generator: an animal model. *J Neurosci*. 2011;31:11256-11267.